

IMAGING OF PHOTONIC QUANTUM RING LASERS BY USING OPTICAL BEAM INDUCED CURRENT MICROSCOPY

Radu HRISTU¹, George A. STANCIU²

Un microscop confocal cu baleaj laser este modifiat pentru a realiza investigații pe un nou tip de laser semiconductor – laserul cu inel cuantic fotonic, folosind tehnica microscopică a fotocurentului indus de radiația laser. Mai exact vom analiza comportamentul structurilor de diferite dimensiuni cu variația tensiunii de polarizare a dispozitivului laser și a puterii laserului de excitație.

A confocal laser scanning microscope is modified to investigate a novel type of semiconductor laser – photonic quantum ring laser, by using the optical beam induced current microscopy technique. Specifically, we analyze the behaviour of the structures with different dimensions when changing the bias of the investigated laser and the excitation laser power.

Keywords: optical beam induced current, semiconductor laser, photonic quantum ring laser

1. Introduction

Photonic quantum ring (PQR) lasers [1] are a novel type of whispering gallery mode lasers with submilliampere threshold currents. This cylindrical vertical-cavity surface-emitting laser (VCSEL)-like structure exhibits a two threshold behaviour of successive lasings. At low bias currents (μ A threshold currents) these devices are lasing only on their circumference – PQR mode, without any intentionally fabricated ring structure; at mA threshold currents there is the usual VCSEL lasing mode [2].

PQR laser devices need a non-destructive optical and electrical investigation technique in order to be characterized with good spatial resolution. The most suited one is the optical beam induced current (OBIC) microscopy that has found wide-spread applications in characterizing many semiconductor and optoelectronic devices [3]. The working principle for the OBIC microscopy involves focusing a laser source onto the sample by using an objective lens and scanning it over the sample. If the photon energy is higher than the band-gap of

¹ PhD student, Faculty of Electronics, Telecommunications and Information Processing, University POLITEHNICA of Bucharest, Romania, e-mail: hristu_radu@yahoo.com

² Prof., Dept. of Physics, University POLITEHNICA of Bucharest, Romania

the semiconductor under investigation, electron-hole pairs are generated. When created in the space charge region they are immediately separated by the electric field and collected by the electrodes to form a current that can be measured. The contrast mechanism that creates the OBIC image is this generated photocurrent that is collected and measured.

OBIC has been used to characterize diodes and determine carrier lifetime [4] or estimate the diffusion length of carriers in photovoltaic devices [5]. Photonic devices have also been investigated by using OBIC imaging: the uniformity and the quantum efficiency of the active region for semiconductor laser diodes [6, 7] and VCSELs [8]. Comparisons between OBIC imaging and photoluminescence (PL) imaging have been made when characterizing light emitting diodes [9, 10] and it has been shown that when the two have the same origin the OBIC image is more sensitive and specific than the PL.

We have previously reported investigations on PQR lasers by using the OBIC microscopy technique when employing a HeNe laser with a 633nm wavelength [11] and also we have made a comparison between lasing profiles and OBIC images [12].

In this study we investigate the response of PQR lasers under reverse and forward biases using the OBIC method. We compare the OBIC images with the confocal reflection images and try to explain the origin of the photoinduced current. Additionally, the response of the structures under different excitation laser powers is analyzed.

2. Experimental

PQR devices of various diameters were grown on a single chip on n-type (100) GaAs substrate by metal-organic vapor-phase epitaxy method. The structure (fig. 1) consists of two DBR mirrors surrounding a one- λ cavity, which has three 8 nm GaAs quantum wells, $Al_{0.3}Ga_{0.7}As$ barriers and spacers. The thickness of the active region is 269.4 nm. There are 38.5 periods in the n-type bottom mirror and 21.5 periods in the p-type top mirror. The mirrors consist of alternating 41.98 nm $Al_{0.15}Ga_{0.85}As$ and 48.82 nm $Al_{0.95}Ga_{0.05}As$ layers. Between the layers, a 20 nm thick linearly graded $AlGaAs$ layer was grown. The p- and n-DBR mirrors were doped with C and Si, respectively. The thicknesses of the quantum wells and their compositions are tuned to yield a resonance wavelength of 850 nm in the vertical direction.

Cylindrical mesas with a height of 5.5 μm are structured by chemically assisted ion-beam etching and are planarized by polyimide in order to connect a stripe electrode. More details regarding the fabrication of similar structures can be found in [13].

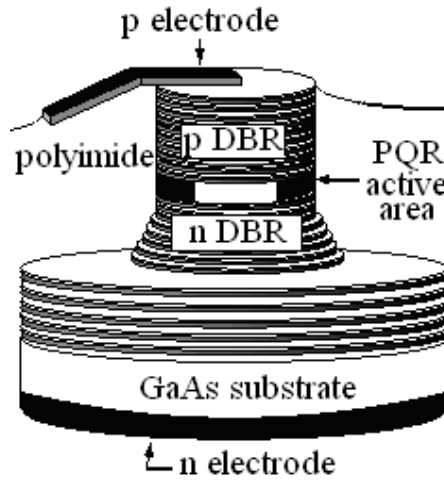


Fig. 1. Diagram of a cylindrical PQR laser structure.

The OBIC experimental setup was developed based on a commercial Leica TCS SP confocal laser scanning microscope (CLSM). This system has the advantage that it can simultaneously obtain confocal (reflection) and OBIC images. A HeNe laser (633 nm) provides the excitation source. A 10X, 0.4 NA objective was used to optimize the spatial resolution, the field of view and the working distance. For OBIC imaging, the photocurrent signal (in the range of tens of nA) is pre-conditioned by a current preamplifier (SR-570, Stanford Research) before being fed into the synchronized A/D converter of the CLSM.

In order to evaluate the photocurrent generated by the PQR lasers we have used the freely distributed software application *ImageJ* [<http://rsbweb.nih.gov/ij/>] to analyze the OBIC images.

3. Results and discussions

OBIC and reflection images were simultaneously acquired (fig. 2) from different PQR lasers. In the case of such a device one would expect to have an uniform distribution of carriers in the active plane of the structure, hence a uniform OBIC image of the PQR laser structure. When overlapping the two images it is clear that there is a non-uniform distribution of the generated photocurrent in the PQR active area. The maximum photocurrent intensity comes from the circumference of the cylindrical structure, the central region showing a lower intensity of the generated photocurrent. This different behaviour of the central and peripheral regions is investigated in detail when we applied forward and reverse biases on the PQR lasers and collected the corresponding OBIC images. The excitation laser power is also varied to see its effect on the distribution of the OBIC across the investigated devices.

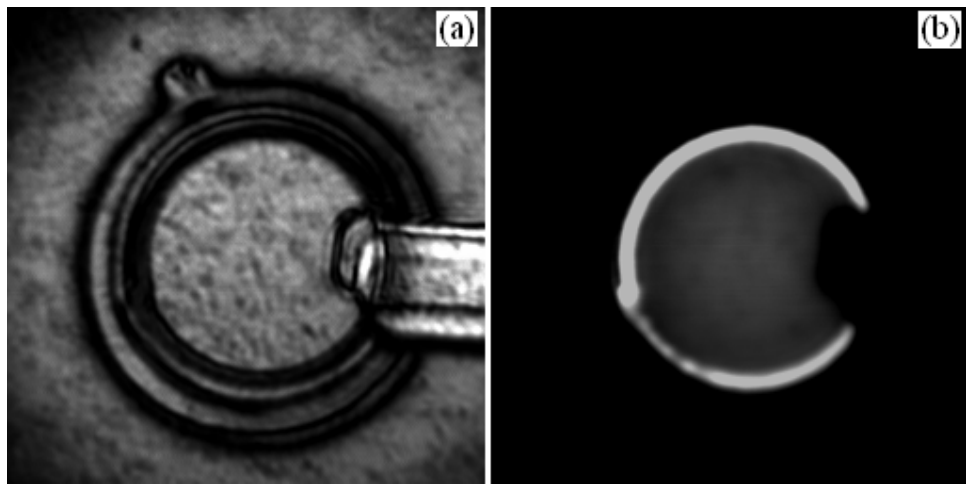


Fig. 2. Reflection image and corresponding OBIC image of a 32 μm diameter PQR laser.

Typical sets of OBIC images under forward and reverse bias are shown in figs. 3 and 4, respectively.

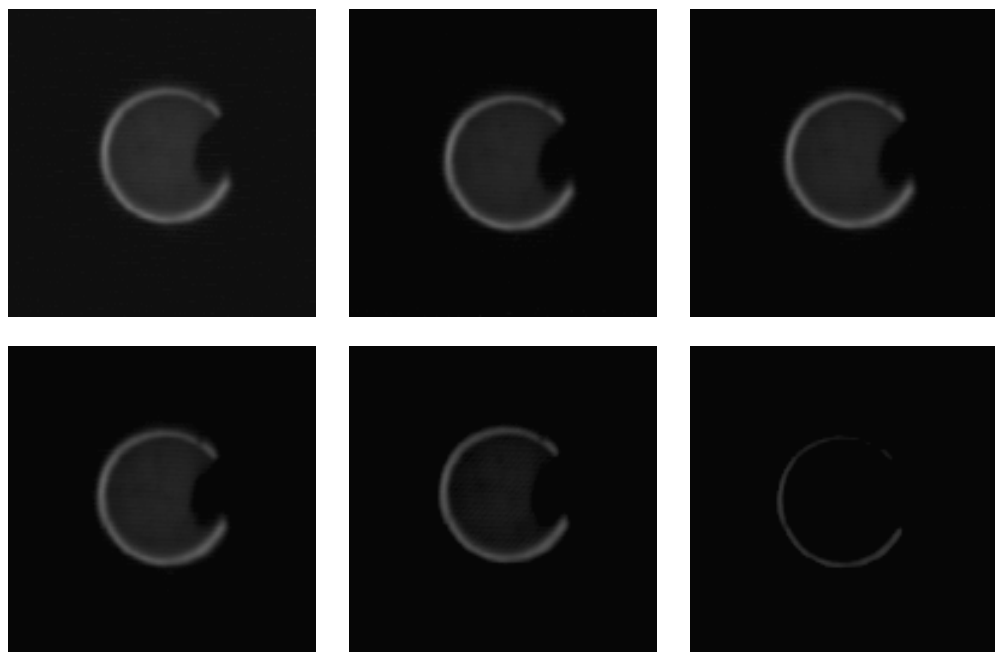


Fig. 3. OBIC images of a 29 μm diameter structure at different forward biases. The first image is taken at 0 V and then the bias is increased in steps of 0.2 V. When the voltage is increased over 1 V no photocurrent is detected. The scanning window for each image is 70 $\mu\text{m} \times 70 \mu\text{m}$. Excitation laser power is kept constant at 50 μW at the sample surface.

We first analyze the OBIC images by forward biasing the PQR laser and varying the voltage from 0 to 1.2 V. We find that the intensity of the photocurrent generated in the central region of the PQR laser under forward bias is very low. For the peripheral region the photocurrent remains almost constant when the bias increases from 0 V to 0.6 V. It then diminishes rapidly and is beyond detection at over 1 V. The same behaviour can be observed on PQR lasers of different diameters.

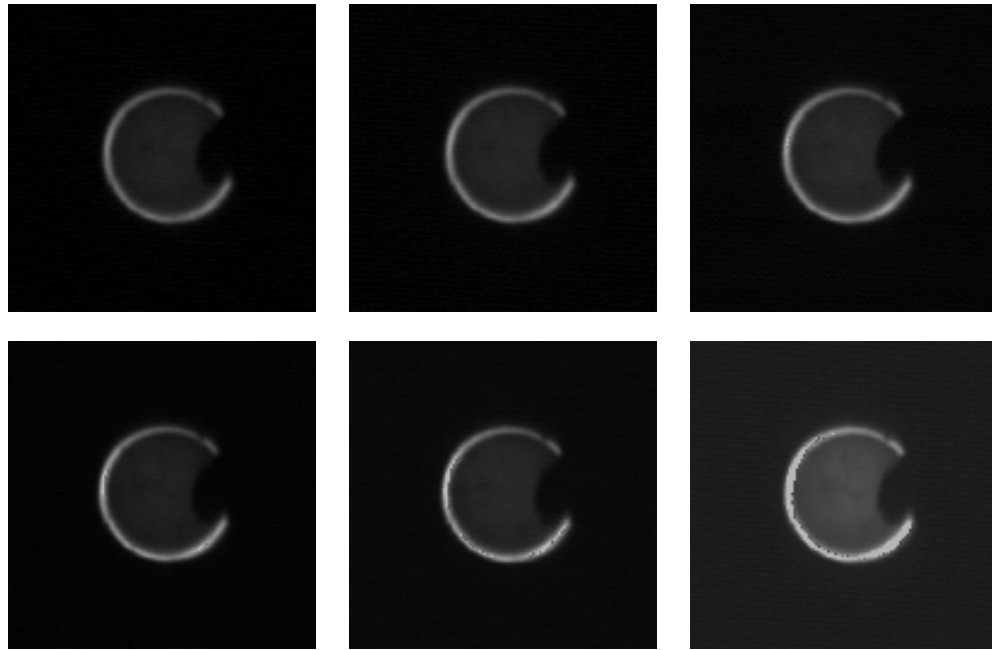


Fig. 4. OBIC images of a 29 μm diameter structure at different reverse biases. The first image is taken at 0 V and then the bias is increased in steps of 2 V. The scanning window for each image is 70 $\mu\text{m} \times 70 \mu\text{m}$. Excitation laser power is kept constant at 50 μW at the sample surface.

In comparison with the forward bias situation, we noted that under reverse bias the PQR laser is effectively a detector and the OBIC signal increases with the bias. For the central region the same situation as for the case of forward biasing is observed: a low intensity photocurrent is generated, this time increasing with the reverse bias. By applying a reverse bias to the *pn* junction, the intrinsic potential barrier (depletion layer) is increased by an energy that is proportional to the bias voltage. The expansion of the depletion layer allows more efficient absorption of photons as well as higher carrier collection efficiency. At higher reverse biases the noise also increases due to a carrier generation outside the structures, hence the higher intensity of the background in the OBIC image corresponding to a 10 V reverse bias (fig. 4).

The response curves (figs. 5 and 7) at three different excitation powers for both the central region and the peripheral ring of the PQR laser show a nonlinear dependence of the generated photocurrent intensity for forward as well as reverse biases.

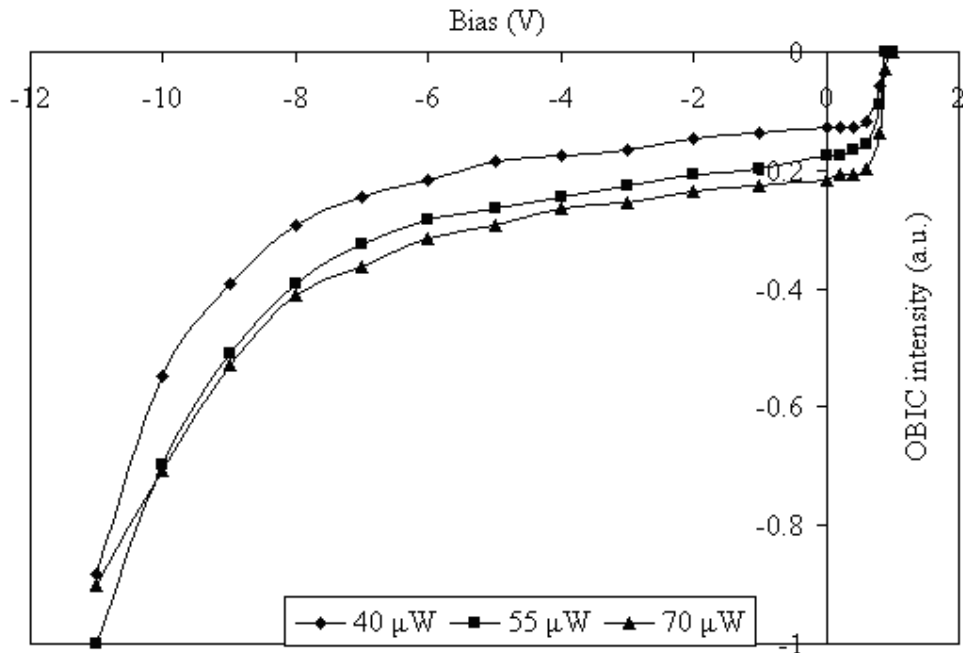


Fig. 5. OBIC intensity as a function of bias for the central region of the PQR laser for three different excitation powers.

The photodiode-like behaviour of the central region is further demonstrated by the OBIC intensity dependence with the excitation laser power (fig. 6); an increase in laser power leads to an increase in the absolute value of the photocurrent as expected in the case of an usual photodiode.

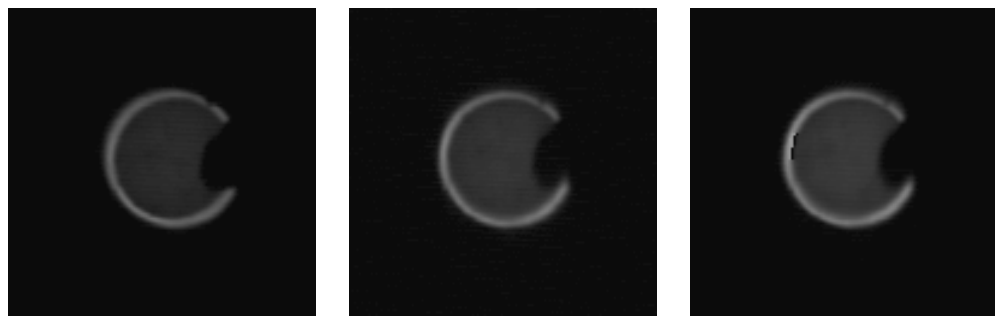


Fig. 6. OBIC images at different excitation laser powers (40 μ W, 55 μ W, 70 μ W).

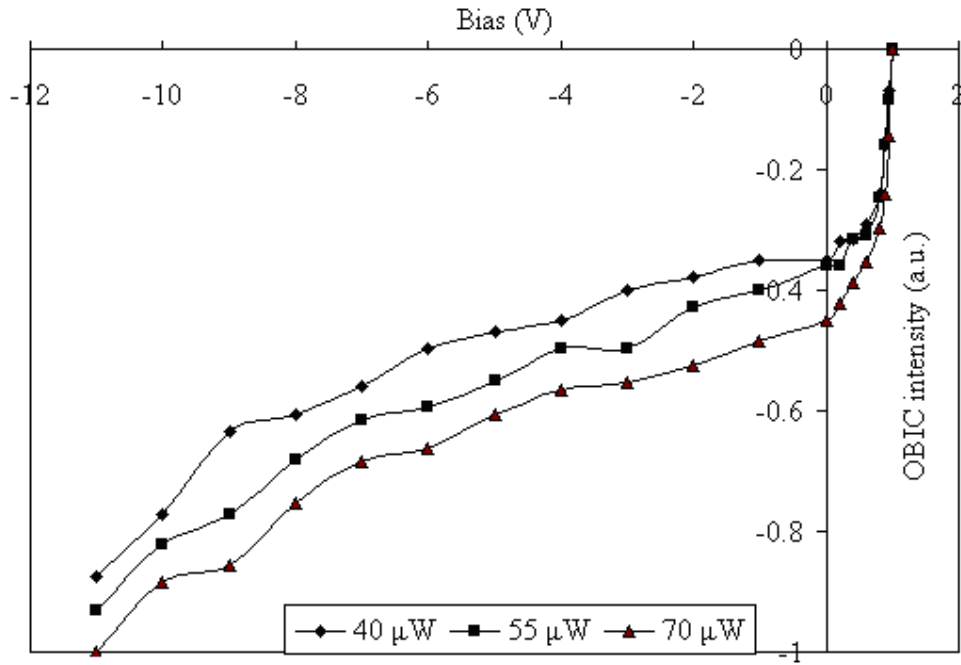


Fig. 7. OBIC intensity as a function of bias for the peripheral ring of the PQR laser for three different excitation powers.

For the peripheral ring at forward bias we can see the same decrease in OBIC from 0 to 1 V. An almost linear increase in the photocurrent intensity at reverse biases (fig. 7) denotes a different behaviour of the peripheral region compared to the central region of the same PQR laser.

4. Conclusions

By using optical beam induced current microscopy we were able to investigate photonic quantum ring lasers and to highlight a different behaviour of the central region as compared to the peripheral region. This different behaviour can be connected with the two lasing modes that the PQR lasers exhibit when electrically pumped. By analyzing the response curves of the lasers at different excitation powers and under reverse and forward bias we noticed a similar behaviour of the two regions under forward bias. Under reverse bias the difference between the two regions was highlighted. Different diameter structures show similar behaviour under the investigated parameters. OBIC studies on PQR lasers could help at understanding the carrier-photon coupling and the physics behind these devices.

R E F E R E N C E S

- [1] *J. C. Ahn, K. S. Kwak, B. H. Park, H. Y. Kang, J. Y. Kim and O'D. Kwon*, "Photonic Quantum Ring", Phys. Rev. Lett., **vol. 82**, no. 3, Jan. 1999, pp. 536-539
- [2] *J. C. Ahn, H. Y. Kang and O'D. Kwon*, "Angle-dependent multiple-wavelength radial emissions in a toroidal microcavity", Proc. of SPIE, **vol. 3283**, 1998, pp. 241-251
- [3] *F.-J. Kao, J.-C. Chen, S.-C. Shih, A. Wei, S.-L. Huang, T.-S. Horng, P. Torok*, "Optical beam induced current microscopy at DC and radio frequency", Opt. Commun., **vol. 211** Oct. 2002, pp. 39-45
- [4] *C. Raynaud, S.-R. Wang, D. Planson, M. Lazar and J.-P. Chante*, "OBIC analysis for 1.3 kV 6H-SiC p+n planar bipolar diodes protected by junction termination extension", Diam. Relat. Mat., **vol. 13**, no. 9, Sep. 2004, pp. 1697-1703
- [5] *Y. Sayad, A. Kaminski, D. Blanc, A. Nouiri and M. Lemiti*, "Determination of diffusion length in photovoltaic crystalline silicon by modelisation of light beam induced current", Superlattices Microstruct., **vol. 45**, no. 4-5, Apr.-May 2009, pp. 393-401
- [6] *G. Stanciu and D. Botez*, "Investigation on Al-free laser quantum-well semiconductor structure by LSM", Microscopy and Analysis, **vol. 88**, 2002, pp. 5-6
- [7] *A. Richter, J. W. Tomm, Ch. Lienau and J. Luft*, "Optical near-field photocurrent spectroscopy: A new technique for analyzing microscopic aging processes in optoelectronic devices", Appl. Phys. Lett., **vol. 69**, no. 26, Dec. 1996, pp. 3981-3983
- [8] *J.W. Tomm, T. Gunther, Ch. Lienau, A. Gerhardt and J. Donecker*, "Near-field photocurrent spectroscopy of laser diode devices", J. Cryst. Growth, **vol. 210**, no. 1-3, Mar. 2000, pp. 296-302
- [9] *F.-J. Kao, M.K. Huang, Y.S. Wang, S.L. Huang, M.K. Lee and C.K. Sun*, "Two-photon optical-beam-induced current imaging of indium gallium nitride blue light-emitting diodes", Opt. Lett., **vol. 24**, no. 20, Oct. 1999, pp. 1407-1409
- [10] *E. Esposito, F.-J. Kao and G. McConnell*, "Confocal optical beam induced current microscopy of light-emitting diodes with a white-light supercontinuum source", Appl. Phys. B **vol. 88**, no. 4, Sept. 2007, pp. 551-555
- [11] *G.A. Stanciu, R. Hristu, S.G. Stanciu, O'D. Kwon and D.K. Kim*, "Optical induced current technique used to investigate the photonic quantum ring laser", Proc. of 2010 ICTON, Munich, Germany (2010)
- [12] *R. Hristu, S.G. Stanciu, S.J. Wu, F.-J. Kao, O'D. Kwon and G.A. Stanciu*, "Optical beam induced current microscopy of photonic quantum ring lasers", Appl. Phys. B, **vol. 103**, no. 3, Jun. 2011, pp. 653-657
- [13] *J. Y. Kim, K. Y. Kwak, J. S. Kim, B. Kang and O'D. Kwon*, "Fabrication of photonic quantum ring laser using chemically assisted ion beam etching", J. Vac. Sci. Technol. B, **vol. 19**, no. 4, Jul.- Aug. 2001, pp. 1334-1338.